

## Study of the Levels in $^{140}\text{La}$ by $(d,p)$ Stripping Reaction\*

JEAN KERN†, GORDON L. STRUBLE, AND RAYMOND K. SHELINE

*Departments of Chemistry and Physics, Florida State University, Tallahassee, Florida and  
Department of Chemistry and Lawrence Radiation Laboratory, University of California, Berkeley, California*

(Received 13 June 1966)

The energy levels in  $^{140}\text{La}$  were studied by means of  $(d,p)$  reaction spectroscopy using 10-MeV deuterons. The protons that emerged were analyzed by a single-gap, broad-range magnetic spectrograph with 13-keV resolution. We obtained the reaction  $Q$  value of  $2938 \pm 3$  keV. Exposures were taken at eight angles ranging from  $25^\circ$  to  $105^\circ$ . All spectra were fitted, using a least-squares code, up to an excitation energy of 1860 keV. Seventy states were observed and the angular distributions of the most prominent groups were analyzed by means of distorted-wave Born-approximation stripping theory. Spins of the  $^{140}\text{La}$  levels determined from previous decay-scheme studies and the present research, and the proton intensities observed in the  $^{139}\text{La}(d,p)^{140}\text{La}$  reaction, can be satisfactorily explained in terms of the mixed configurations,  $(1g_{7/2})_p(2f_{7/2})_n$  and  $(2d_{5/2})_p(2f_{7/2})_n$ . Above 600 keV, however, interpretation of states in terms of higher energy configurations appears also to require phonon-particle coupling.

### I. INTRODUCTION

AMONG the different nuclear species, odd-odd nuclei are perhaps the most difficult to study. From the experimental point of view, this is true for several reasons. Frequently the mass of a particular odd-odd nucleus is greater than that of both its neighboring even-even isobars. This makes it impossible to observe levels in the odd-odd nucleus by beta-ray and gamma-ray spectroscopy. In the case where levels in an odd-odd nucleus can be populated by beta decay, the daughter nucleus itself is usually unstable and this situation demands difficult experimental techniques for the spectroscopist. Finally the decay occurs from a state with  $0+$  spin and parity and only states with small spins will be observed. In principle, reaction spectroscopy offers a means of observing more states in odd-odd nuclei but the high level density in heavier odd-odd nuclei creates an obstacle because usually the experimental resolution is ten to one hundred times poorer than that obtainable with beta- and gamma-ray studies.

Interpreting the experimental levels in odd-odd nuclei is also difficult because simple phenomenological models inadequately describe the low-energy spectra. The ordering of the levels in the multiplets resulting from a specific neutron and proton configuration is sensitive to the nature of the neutron-proton residual interaction. However, it is just this feature which makes the study of odd-odd nuclei so important, since the detailed level structure can then give information about this interaction.

Although odd-odd nuclei near magic configurations have been studied in detail,<sup>1</sup> little work has been

attempted either in deformed nuclei<sup>2,3</sup> or in the so-called vibrational nuclei. In this and in the following paper we examine the nucleus  $^{140}\text{La}$ , a nucleus with one neutron outside the 82 shell and 7 protons outside the 50 shell. Experimentally this is a favorable nucleus for nuclear-reaction studies because  $^{139}\text{La}$  is stable, nearly monoisotopic, and the reaction  $^{139}\text{La}(d,p)^{140}\text{La}$  has a  $Q$  value which makes it possible to study  $^{140}\text{La}$  by this reaction with 10-MeV deuterons. Thus unambiguous data may be obtained using a deuteron beam from a Tandem Van de Graaff accelerator, a natural  $^{139}\text{La}$  target, and a magnetic spectrograph to analyze the reaction products. Theoretically the nucleus is expected to be of intermediate difficulty. That is, although there is extensive configuration mixing due to interactions of the seven protons, it is in a region where quasiparticles which are defined by a special Bogoliubov transformation give good descriptions of even-even and odd- $A$  systems.<sup>4</sup> Also since there is only one neutron outside the 82 magic neutron configuration, one would expect very small vibrational phonon amplitudes in the lower single quasiproton states.<sup>5</sup> It should be possible to describe the states below 1 MeV by an effective quasiproton neutron interaction using an odd-odd quasiparticle model.

In Sec. II, the results of previous experimental investigations are reviewed. In Secs. III and IV, a discussion of the experimental technique and the results from the studies of levels below 1.858 MeV by  $(d,p)$  reaction spectroscopy are given. A qualitative discussion of the odd-odd quasiparticle model is presented in Sec. V and an interpretation of our levels below 600 keV is given. In the second paper we give the mathematical details of the odd-odd quasiparticle model and apply this model to  $^{140}\text{La}$ .

\* This work was supported in part by the U. S. Atomic Energy Commission under Contract No. W-7405-eng-48 and AT-(40-1)-2434. The Florida State University Tandem Van de Graaff was supported by the U. S. Air Force Office of Scientific Research under Contract No. AFOSR-62-423 and by the Nuclear Program of the State of Florida. Supported in part by the Fonds National Suisse de la Recherche Scientifique.

† Present address: Physics Department, University of Fribourg, Fribourg, Switzerland.

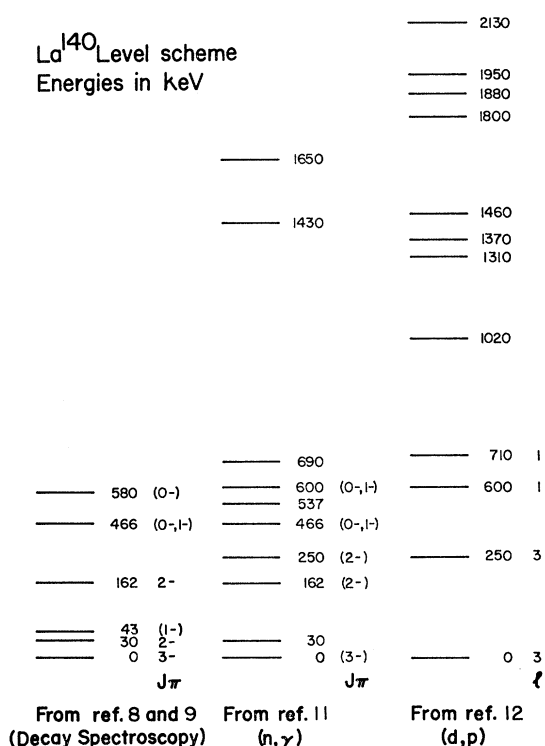
<sup>1</sup> Y. E. Kim, University of California Radiation Laboratory Report No. UCRL-10865 (unpublished).

<sup>2</sup> G. L. Struble, J. Kern, and R. K. Sheline, Phys. Rev. **137**, B772 (1965).

<sup>3</sup> G. L. Struble and J. O. Rasmussen, Phys. Letters **17**, 283 (1965).

<sup>4</sup> L. S. Kisslinger and R. A. Sorensen, Rev. Mod. Phys. **35**, 853 (1963).

<sup>5</sup> See wave functions for  $^{139}\text{La}$  and  $^{141}\text{Ce}$  in Kisslinger and Sorensen (Ref. 4).

FIG. 1. Levels in  $^{140}\text{La}$  known from previous investigations.

## II. PREVIOUS INVESTIGATIONS

The investigation of the beta decay of  $^{140}\text{Ba}$  to  $^{140}\text{La}$  has been performed by many different groups.<sup>6</sup> The high-resolution work of Geiger, Graham, and Ewan<sup>7</sup> strongly suggested a number of spin-parity assignments and accurate energy levels. These assignments have been confirmed by the gamma-gamma angular correlation measurements of Agarwal *et al.*<sup>8</sup> and lifetime measurements of Burde *et al.*<sup>9</sup> Burde *et al.* confirmed the original level assigned by Geiger *et al.* at 581.1 keV which had been reassigned at 566 keV by Agarwal *et al.*

A level scheme consistent with these results is given in Fig. 1. Low-energy gamma rays from thermal-neutron capture<sup>10</sup> could not be placed consistently in the existing scheme but the study of high-energy gamma rays following neutron capture<sup>11</sup> defined some additional new levels. (See Fig. 1.) Study of  $^{140}\text{La}$  by the  $(d,p)$

<sup>6</sup> *Nuclear Data Sheets*, compiled by K. Way *et al.* (Printing and Publishing Office, National Academy of Sciences—National Research Council, Washington, D. C.).

<sup>7</sup> J. S. Geiger, R. L. Graham, and G. T. Ewan, *Bull. Am. Phys. Soc.* **6**, 71 (1961); (private communication).

<sup>8</sup> Y. K. Agarwal, C. K. Baba, and S. K. Bhattacharjee, *Nucl. Phys.* **58**, 641 (1964).

<sup>9</sup> J. Burde, M. Rakavy, and G. Adam, *Nucl. Phys.* **68**, 561 (1965).

<sup>10</sup> M. Giannini, G. Pinto, D. Prospero, and S. Sciuti, *Nuovo Cimento* **29**, 977 (1963).

<sup>11</sup> L. V. Groshev, A. M. Demidov, and V. I. Pelekhov, in *Soviet Progress in Neutron Physics*, edited by P. A. Krupchitskii (Consultants Bureau, Inc., New York, 1963), p. 248.

stripping reaction was performed by Bingham and Sampson<sup>12</sup> with an energy resolution of approximately 70 keV. Angular distributions were measured and the  $l$  transfers were determined for a few groups. Comparison of these results with the decay-scheme results (Fig. 1) shows that the resolution was not good enough to resolve some of the known states. Since our instrumentation is appreciably better in this respect, a re-investigation of the reaction seemed worthwhile.

## III. EXPERIMENTAL METHOD

Targets were prepared by evaporating  $\text{La}_2\text{O}_3$ <sup>13</sup> from a small carbon crucible under a high vacuum onto thin carbon backings. The required temperature was achieved by using an electron-gun technique.<sup>14</sup> The backings were obtained by depositing carbon by an electric arc in a high vacuum onto glass slides that had previously been coated with Teepol (a product of Shell research). After  $^{139}\text{La}$  was evaporated, the target was floated on de-ionized water and mounted on an aluminum frame. Targets prepared by this method have a thickness of approximately  $100\ \mu\text{g}/\text{cm}^2$  and the carbon backings a thickness of  $10\text{--}30\ \mu\text{g}/\text{cm}^2$ .

The targets were then exposed to the 10-MeV deuteron beam of the Florida State University Tandem Van de Graaff. This beam was collimated by  $\frac{1}{4}\times 3$  mm slits before reaching the target and the Faraday cup. The emerging protons were analyzed in a single-gap magnetic Browne-Beuchner spectrograph.<sup>15</sup> The solid angle of this spectrograph is of the order of  $0.7\times 10^{-4}$  sr. As a detector we used an array of three  $5\times 25$  cm  $50\text{-}\mu$ -thick nuclear-emulsion plates which are manufactured by Eastman Kodak Company. These plates were covered with an aluminum foil 0.12 mm thick in order to stop elastically scattered deuterons. After exposure, the proton tracks were counted in  $\frac{1}{2}$  mm strips under microscopes equipped with calibrated stages. A more detailed description of this general experimental procedure is given in a recent publication by Kenefick and Sheline.<sup>16</sup>

The resulting spectrum was analyzed by use of a nonlinear least-squares code<sup>17</sup> in order to determine the individual components of the spectrum. This method of analysis was necessary because many of the peaks were unresolved. The shape of the line profile and the linewidth were inferred from the most prominent peaks. This resulted in a profile with a symmetric Gaussian curve that has a small low-energy tail (approximately

<sup>12</sup> F. W. Bingham and M. B. Sampson, *Phys. Rev.* **128**, 1796 (1962).

<sup>13</sup> High-purity  $\text{La}_2\text{O}_3$  was provided by Johnson, Matthey and Company, London.

<sup>14</sup> M. C. Oleson and B. Elbek, *Nucl. Phys.* **15**, 26 (1960).

<sup>15</sup> C. P. Browne and W. W. Buechner, *Rev. Sci. Instr.* **27**, 899 (1956).

<sup>16</sup> R. A. Kenefick and R. K. Sheline, *Phys. Rev.* **133**, B25 (1964).

<sup>17</sup> R. H. Moore and R. K. Zeigler, Atomic Energy Commission Report No. LA-2367 (unpublished).

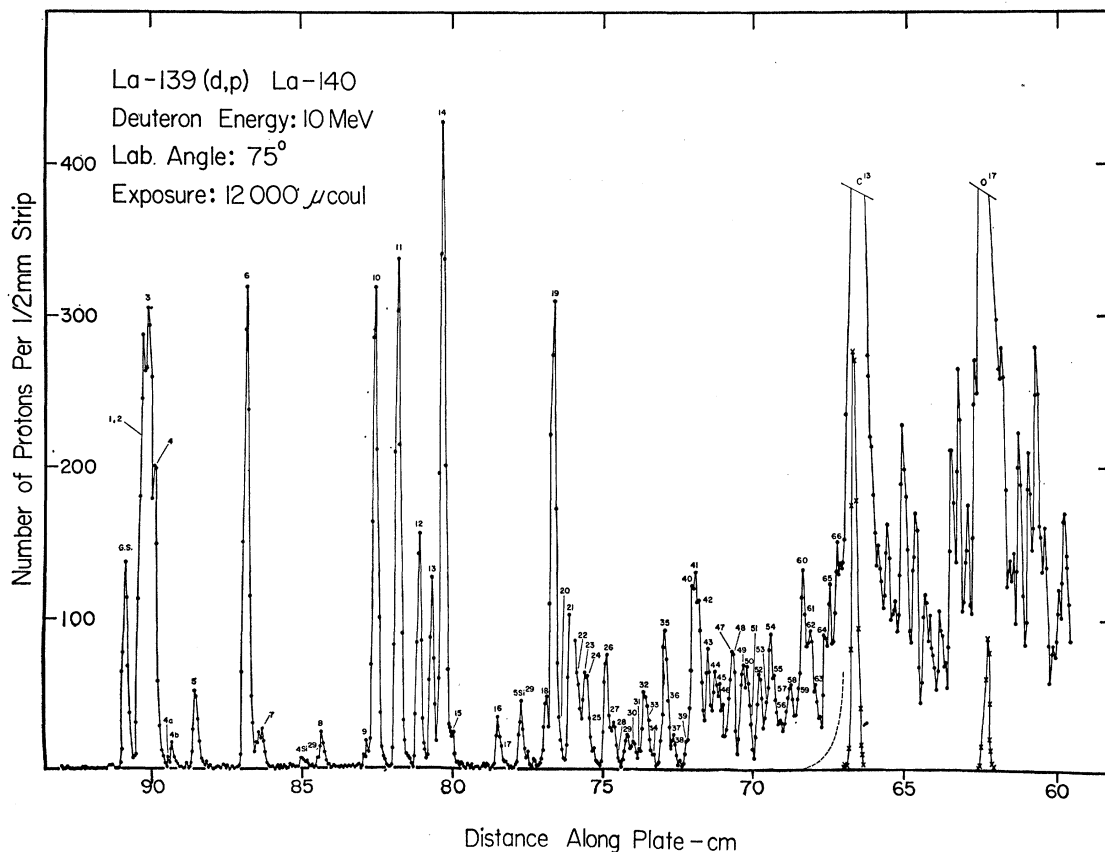


Fig. 2. Typical proton spectrum for the reaction  $^{139}\text{La}(d,p)^{140}\text{La}$ .

5% of the total intensity) which was, in general, neglected.

The position of the peaks, as determined by the least-squares analysis, was then entered in a code written for an IBM 709 in order to extract  $Q$  values and excitation energies. This code used an empirical energy calibration and determined whether any of the entered peaks could be due to reaction with one of the impurities that might have contaminated the target. Such impurities could come from the Teepol, the glass slide, or possibly from the tungsten filament of the electron gun.

Calculations of the average, weighted average, and corrected average of the excitation energies were made. As a weight a quantity approximately inversely proportional to the square of the standard deviation of the peak position, as determined by the least-squares code, was used. In the corrected average, values whose dispersions were greater than five times the standard deviation for a single value were discarded.

In order to obtain meaningful angular distributions, either we needed to determine absolute cross sections or to ensure that the target thickness and the luminosity of the spectrograph remained unchanged at the different angles. We chose the first method. To obtain absolute cross sections, we bombarded the target at each angle

with 4-MeV deuterons prior to and/or after the  $(d,p)$  experiment assuming that the same geometrical configuration was maintained at the spectrograph. (In fact the aluminum foil covering the emulsion plates had to be removed for this experiment.) From the known Rutherford cross section, it was then a straightforward procedure to obtain the absolute cross sections.

#### IV. RESULTS

Eight exposures were taken at angles ranging from  $25^\circ$  to  $105^\circ$ . Table I gives a summary of some of the details of the experiments. The resolution given here is the full width at half-maximum of the ground-state

TABLE I. A summary of experiments.

Target No.	Angle (deg)	Exposure ( $\mu\text{C}$ )	Resolution (keV)	Cross section/track ( $\mu\text{b}/\text{sr}$ )	$Q$ value (keV)
1	25	10 000	13.1	0.20	2939.7
3	35	6000	12.4	0.56	2936.4
3	45	7500	12.8	0.45	2939.1
3	55	6000	13.9	0.54	2939.1
3	65	6000	12.1	0.58	2938.5
3	75	12 000	12.8	0.29	2937.6
4	85	9000	14.3	0.13	2921.1
6	105	8000	12.1	0.32	2937.8

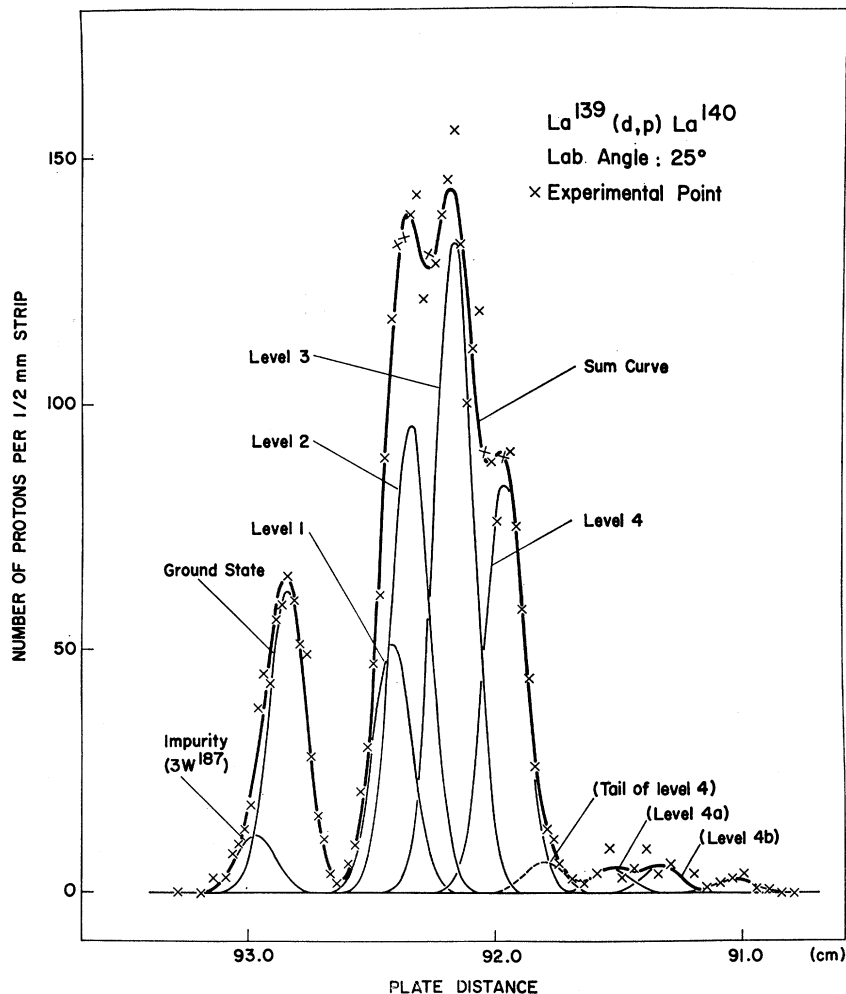


FIG. 3. Least-squares fit of the high-energy part of the  $25^\circ$  proton spectrum from the reaction  $^{139}\text{La}(d,p)^{140}\text{La}$ .

peak. It was found that the energy resolution decreases slowly along the plates when going toward smaller proton energies. For example, it is about 3 keV larger at 1800-keV excitation than at the ground state. The differential cross section corresponding to one track is given as a measure of the ultimate sensitivity in a particular exposure. This quantity, together with the exposure, gives some indication about the relative target thickness. We see, for instance, that the target used at  $85^\circ$  is appreciably thicker than the others, and this resulted in a broadening of the lines.

When the value at  $85^\circ$  is disregarded, the agreement of  $Q$  values determined at various angles is very satisfactory. The corrected average is  $Q = 2938.3 \pm 0.4$  keV. The good reproducibility of the  $Q$  value, even though the plate distance from the calibration peak (carbon) to the ground-state peak varies considerably, indicates that the systematic error of the calibration is small, and we therefore give the value of

$$Q = 2938 \pm 3 \text{ keV.}$$

This gives a binding energy of the last neutron  $B_n = 5.163 \pm 0.004$  MeV.

Our experimental number is in disagreement with and outside the experimental error of Everling *et al.*,<sup>18</sup> who give the value  $B_n = 5.021 \pm 0.07$  MeV. It is considerably closer to the value of  $5.145 \pm 0.015$  MeV determined in the  $(n,\gamma)$  work of Groshev *et al.*<sup>11</sup> and the value of 5.11 MeV derived from the  $(d,p)$   $Q$  value of Bingham and Sampson.<sup>12</sup> In view of the high resolution available and the internal consistency of these experiments, we believe that the  $B_n$  value reported here is the most accurate.

A typical spectrum is displayed in Fig. 2. The exact position of the intense  $^{13}\text{C}$  and  $^{17}\text{O}$  peaks are obtained by short exposures made before and after the main experiment. These peaks are used to recalibrate the incident energy and test the stability of the magnet. They appear outside the range of interest at backward angles, but fall inside it at angles less than  $80^\circ$ . As their cross sections are also much larger at forward angles, it is necessary to subtract a background from under the peaks lying close to them. Because of the large level

<sup>18</sup> F. Everling, L. A. König, J. H. E. Mattauch, and A. H. Wapstra, *Nucl. Phys.* **18**, 529 (1960).

TABLE II. Level energies (keV) and differential cross sections ( $\mu\text{b}/\text{sr}$ ). The standard deviation is given beneath each value.<sup>a</sup>

Level	Energy	Differential cross section								Comments
		25°	35°	45°	55°	65°	75°	85°	105°	
G.S.	0.0	52	134	147	171	194	163	114	96	
		6	9	9	13	15	11	7	11	
1	30.6	43	85	220	149	227	189	147	114	b
	0.2	54	47	56	82	84	54	88	46	
2	37.5	81	265	215	345	243	195	169	157	b
	0.4	47	43	41	59	57	40	95	64	
3	49.2	111	290	448	395	378	325	251	230	b
	0.3	10	17	31	27	50	28	14	13	
4	63.2	70	152	299	277	264	228	199	156	
	0.2	6	9	19	22	18	13	15	11	
4a	92.8	4	4	9	13	11	3	32	5	c
	1.5	1	2	3	4	5	2	4	1	
4b	106.3	5	12	20	13	9	16	30	14	c
	0.7	1	2	2	4	4	3	3	2	
5	161.6	25	44	89	77	71	62	60	43	d
	0.3	2	4	8	7	6	4	5	4	
6	284.2	123	315	477	492	447	387	341	234	
	0.4	8	20	27	30	25	20	17	22	
7	319.2	14	21	40	31	40	35	38	32	
	0.7	1	3	4	4	3	5	3	4	
8	466.6	22	34	35	31	26	20	16	16	WA <sup>e</sup>
	1.0	3	2	3	3	2	4	3	3	
9	578.6	20	39	19	16	14	21	6	6	d
	1.4	3	6	5	3	2	2	3	3	
10	601.6	423* <sup>f</sup>	369	423	431	417	363	263	148	WA, <sup>g</sup>
	0.6	30	25	30	30	25	20	20	14	
11	658.3	374*		488	471	445	373	238	191	
	0.5	30		30	31	26	22	16	13	
12	711.6	257*		228	268	200	162	108	85	
	0.7	25		15	19	14	11	7	7	
13	744.5	184*	188*	191	157	153	117	95	70	
	0.7	20	20	14	12	11	9	6	5	
14	771.7	513*	499*	660	557	492	476	330	237	
	0.6	60	40	38	35	28	26	18	15	
15	794.2	58*	75*	31	35	43	31	68	14	
	0.8	20	10	8	4	5	3	5	2	
16	912.6	40*	75*		33	36	34	23	22	
	0.8	15	20		4	3	4	3	2	
17	930.3	18*	29*		4	8	4	11	8	
	0.8	10	10		1	1	2	2	3	
18	1035.8	47*	54	60	32	41	42	22	17	
	0.6	10	6	6	4	5	5	2	2	
19	1056.9	248	349	339	370	351	326	228	154	h
	0.8	20	23	24	23	21	20	13	9	
20	1076.9	23	33	28	17	14	21	24	5	
	1.4	3	5	4	4	4	5	2	1	
21	1102.4	124	147	157	161	151	149	111	62	
	0.9	10	13	11	10	11	14	7	6	
22	1118.2	70	80	79	79*	75	55	75	27	i
	0.9	8	8	7	15	7	5	5	5	
23	1137.0	80	108	108	75*	75	55	74	35	WA
	1.0	8	9	8	15	9	13	7	5	
24	1149.9	33*	29	43	67*	26	37	24	29	
	1.4	10	5	6	15	4	14	4	5	
25	1169.1	33*	36	19		8	6	12	3	WA
	1.0	10	4	4		3	1	4	2	

<sup>a</sup> For the significance of these standard deviations, the reader is referred to the paragraph on errors in Sec. IV. Since we cannot make a good estimate of such errors as the energy calibration error at this time, we prefer not to increase arbitrarily the standard deviation to include them, in order not to mask such important errors as an improper number of components in the fitting of a group of peaks. Large and erratic differences compared to the standard deviation between our and other values should however not automatically be interpreted in this sense. For instance, impurities may also alter the results, especially in the case of small peaks. We believe that the standard deviation in intensities is in general a good estimate of the true error. However, in some cases an improper number of components, impurities, and the approximate fitting shape may be the cause of large nonstatistical errors.

<sup>b</sup> It appears from the discussion in Sec. V, that there is an unobserved peak at 43 keV which has a non-negligible intensity. The inclusion of this component would, of course, modify the energies and intensities of the close-lying peaks.

<sup>c</sup> It is possible that the two levels 4a and 4b have only been artificially decomposed and that they represent only one level at about 102 keV.

<sup>d</sup> The appearance of impurity peaks near this level at several angles makes the uncertainty of the values appreciably larger than the quoted standard deviations.

<sup>e</sup> WA: The energy value is a weighted value.

<sup>f</sup> The asterisk denotes that a background has been subtracted from the peak.

<sup>g</sup>  $^{55}\text{Si}^{29}$  component at 45°.

<sup>h</sup>  $^{9}\text{F}^{20}$  at 35° (30  $\mu\text{b}$ ).

<sup>i</sup>  $^{55}\text{Si}^{29}$  at 85°.

<sup>j</sup>  $^{9}\text{F}^{20}$  at 45° (30  $\mu\text{b}$ ).

<sup>k</sup> Ground-state (G.S.)  $\text{O}^{19}$  at 25° (100  $\mu\text{b}$ ),  $^{9}\text{F}^{20}$  at 55°,  $^{55}\text{Si}^{29}$  at 105°.

<sup>l</sup>  $^{55}\text{Si}^{29}$  at 105°.

<sup>m</sup> G.S.  $\text{O}^{19}$  at 35° (20  $\mu\text{b}$ ).

<sup>n</sup>  $^{7}\text{Si}^{29}$  at 25° (10  $\mu\text{b}$ ).

<sup>o</sup>  $^{9}\text{Si}^{29}$  at 25° (300  $\mu\text{b}$ ).

<sup>p</sup>  $^{9}\text{Si}^{29}$  at 35° (170  $\mu\text{b}$ ).

TABLE II (continued).

Level	Energy	Differential cross section								Comments
		25°	35°	45°	55°	65°	75°	85°	105°	
26	1191.8	40*	92	115		87	79	65	58	
	0.8	20	8	8		8	5	4	5	
27	1212.0		28	60		33	30	38	16	j
	1.0		5	7		5	4	3	3	
28	1227.1		26	21		5	5	10	4	
	1.7		5	8		3	3	2	2	
29	1245.6		33	24		29	25	24	23	
	0.6		5	3		4	2	3	3	
30	1262.4		22	31	15*	17	19	19		
	0.6		5	4	10	3	3	2	7	
31	1279.9		25*	27	36*	7	10	13	2	
	0.8		10	3	15	2	3	2		
32	1295.4		38*	48	59*	55	53	38	33	
	1.0		10	5	15	5	5	3	4	
33	1312.5		21*	21	19*	14	14	18	17	WA
	1.4		8	2	10	3	3	2	3	
34	1328.0			13	12	7		11	3	
	2.2			3	7	2		3	2	
35	1343.0				103*	71	70	66	60	
	1.3			111	10	17	11	7	12	
36	1352.2	40*		7	33*	43	38	25	19	WA
	1.0	20			15	16	10	6	2	
37	1370.2	42*		26	43*	27	21	23	20	
	0.9	10		3	8	4	3	4	2	
38	1388.0	105*		18	26	10	2	7	43	k
	1.5	20		3	4	3	1	2	29	
39	1403.3	18*		14	24	23	17	15	25	l
	0.6	10		3	7	4	3	4	27	
40	1418.4	49*		79	139	89	107	73	63	
	0.9	15		6	11	13	13	7	6	
41	1431.5	43*		104	113	127	78	107	109	
	0.5	15		20	9	14	19	9	8	
42	1444.0	17*		56*	71	63	61	49	44	
	1.0	10		25	6	14	26	7	4	
43	1461.1	41*	48*	90*	80	84*	78	67	60	
	0.8	20	20	15	15	9	6	7	5	
44	1479.2	40*	43*	45*	88	113*	57	51	44	m
	0.9	15	20	20	10	20	8	5	5	
45	1493.0		43*	46*	65		36	40	40	
	1.4	18*	20	20	9		10	4	5	
46	1508.0	10	68*		55		25	32	24	
	2.2		30		11		13	8	4	
47	1519.3	23*	48*	74	74		38	44		WA
	0.9	10	20	8	8		4	13		
48	1529.2	30*	24*				70	37	74	WA
	0.6	15	10				5	18	7	
49	1554.6	32*	44*	66	66		64	55	52	WA
	0.6	10	15	19	19		7	4	5	
50	1568.9	21*	39*	42	42		40	54	41	
	0.7	10	15	25	25		11	5	5	
51	1583.6	8*	11*	62	62		27	15		
	2.6	5	5	19	19		13	4		
52	1600.1	45*	81*	86*	37	92*	62	53	39	
	0.9	10	10	30	19	25	5	5	5	
53	1616.6	23*	77*	51*	92	35*	28	25	27	
	1.1	10	10	20	10	20	4	12	4	
54	1630.2	36*	48*	64*	45	85*	77	44	55	
	1.0	10	10	20	8	20	7	8	6	
55	1643.6	31*	37	57*	60*	56*	43	42	35	n
	1.1	7	8	20	8	20	5	6	4	
56	1657.4	22*	42	66*	31*	35*	30	34	27	WA
	1.1	5	5	25	8	7	3	4	3	
57	1672.7	24*	35	39*	64*	33*	35	26	11	
	1.1	6	6	25	20	10	5	3	5	
58	1685.2	48	63	74*	51*	89*	48	51	39	
	0.8	6	7	25	15	10	6	4	6	
59	1702.2	43	50	61*	99*	81*	43	48	32	
	0.8	4	5	10		10	5	5	4	
60	1718.1		117	127		91	118	90	48	
	0.8	102	10	12		28	11	7	16	
61	1730.1	8	63	95		109	53	66	47	
	1.6		35	37		30	20	8	5	

TABLE II (continued).

Level	Energy	Differential cross section								Comments
		25°	35°	45°	55°	65°	75°	85°	105°	
62	1742.1	373	43	97		117	64	49	59	°
	1.2	23	37	15		10	19	7	5	
63	1758.2	45	49	83		70	38	33	31	
	1.0	4	6	12		8	6	6	4	
64	1778.4	55	69	73		87	72*	64	46	
	1.0	5	6	15		9	10	5	7	
65	1794.8	64	82	86		106	87*	73	45	
	0.9	5	22	18		10	15	6	8	
66	1810.4	70	242	69		106	103*	77	66	p
	0.8	5	22	19		11	20	7	9	
67	1826.2	52	56	79	78	97		58	50	
	1.0	4	12	22	13	11		5	5	
68	1844.0	48	52	58	131	82		93	48	
	1.3	6	17	12	15	12		8	13	
69	1858.0	62	97	123	112	120		65	71	
	1.5	8	19	16	13	16		8	13	

density, this subtraction is somewhat arbitrary and so we do not attempt to compute cross sections and errors for small peaks in these areas.

The least-squares technique was essential in order to unfold the first group of peaks. In Fig. 3 the individual components and their sum are compared with the experimental spectrum at 25°. A satisfactory fit can also be found when peak 1 is suppressed. However, the fit is then, in general, not as good, and the linewidth seems too large. Furthermore the correspondence with the levels of Fig. 1 is much better when level 1 is added.

Table II gives the results of the present investigation for energy values and differential cross sections. Below each value we give the standard deviation. For the energies these quantities have been computed from the deviations of the single values from the average value. For the intensities they are statistical sums of the standard deviation calculated by the fitting program, the error for the solid-angle calibration and the error for the Rutherford-scattering experiment which is estimated to be 5%. Systematic errors may arise from an error on the energy calibration, use of an approximate fitting function, which may be especially important in the cases of close multiplets, undetected impurities, and an incorrect number of components in the analysis. With regard to energies, the figures given take into account only the statistical errors. It is therefore expected that the true error can be appreciably larger. It may be assumed that the error due to the calibration amounts to 0.5 keV below 600 keV and 1 keV above. We have been tempted to increase arbitrarily the standard deviation by these amounts in order to avoid discrepancies with more precise measurements. But this would also make it impossible to detect meaningful discrepancies. For example, the energy standard deviation 0.2 keV quoted for level 1 at 30.6 keV is too small when compared with the accurately measured energy of  $29.97 \pm 0.05$  keV. As will be shown in Sec. V, the number of components used in fitting

this region is probably incorrect and the discrepancy supports this view. A biased standard deviation would have masked the difficulty. We will use possible large differences between the values given here and more accurate energy values that can be obtained by gamma-ray measurements to help locate systematic errors. For the levels where a background has been subtracted (denoted with an asterisk), the error is estimated. When a known impurity contributes to the cross section, an estimated value of its contribution is given in the comments when possible.

Although we have analyzed all spectra down to peaks with a few tracks, we have excluded from the table peaks with a cross section of only a few microbarns. Such small peaks may reproduce at many angles with an acceptable energy spread. Nevertheless, we believe that usually it is accidental and that the inclusion of such peaks in the table would only be misleading.

To fit the angular distributions we have used the distorted-wave Born approximation (DWBA) code TSALLY of Bassel, Drisko, and Satchler.<sup>19</sup> We know of no experimental values of the optical-model parameters of  $^{139}\text{La}$  for 10-MeV deuterons. Since  $^{140}\text{La}$  is radioactive, the parameters for  $^{140}\text{La}$  and  $\sim 13$ -MeV protons would be very difficult to determine experimentally. For these reasons we have started with parameters extracted from the work of Perey<sup>20</sup> for protons and of Perey and Perey<sup>21</sup> for deuterons. We varied them slightly in order to fit the  $l=3$  distribution of the first group of peaks [Fig. 4(a)] and simultaneously the  $l=1$  distribution of the peaks 10+13+14. This simultaneous fitting put severe constraints on the possible variations. The fit represented in Fig. 4 was obtained with the parameters given in Table III, using the "independent Saxon plus derivative" option.

<sup>19</sup> R. H. Bassel, R. M. Drisko, and G. R. Satchler, Atomic Energy Commission Report No. ORNL-3240 (unpublished).

<sup>20</sup> F. G. Perey, Phys. Rev. **131**, 745 (1963).

<sup>21</sup> C. M. Perey and F. G. Perey, Phys. Rev. **132**, 755 (1963).

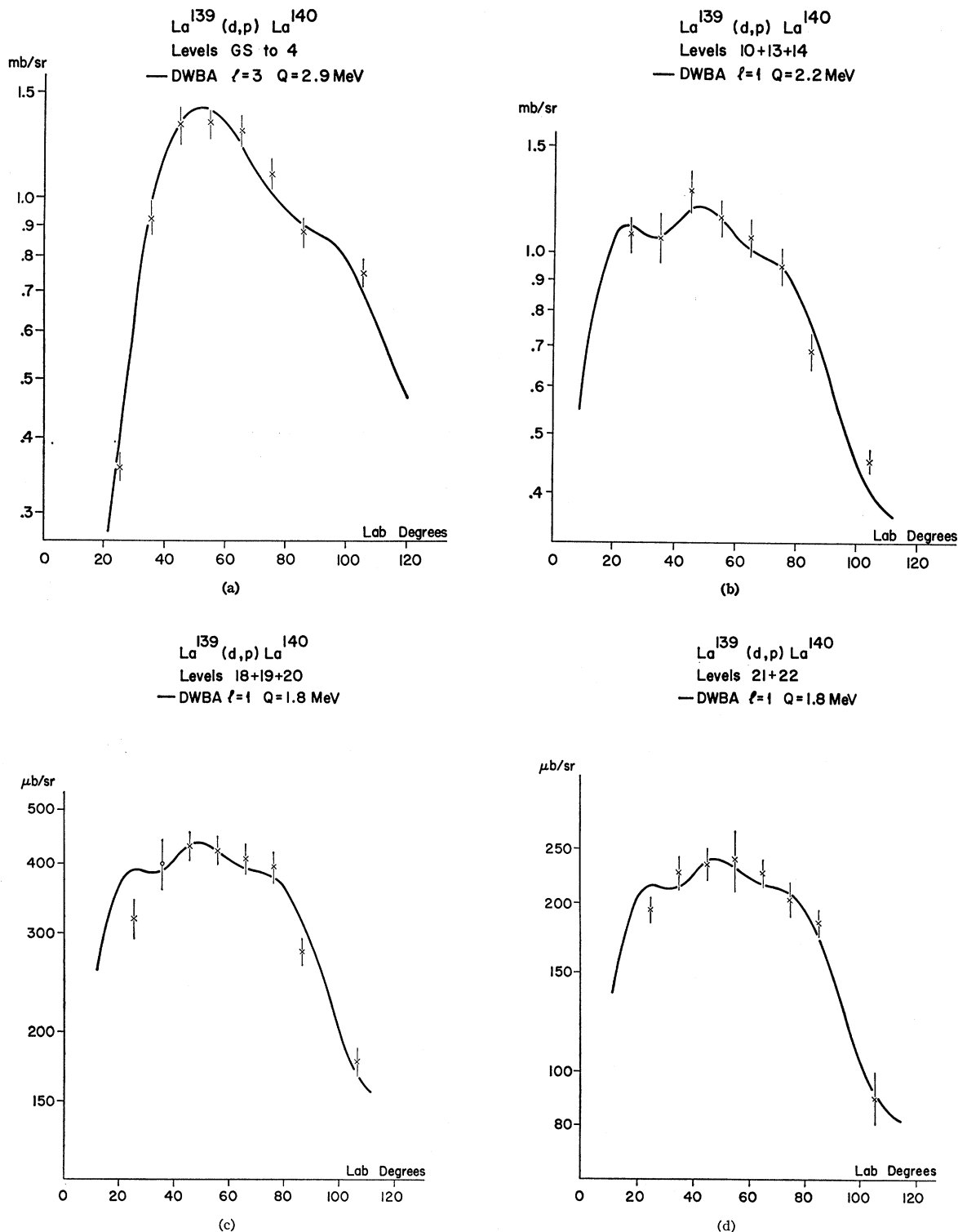


FIG. 4. Angular distribution of several different proton groups from the reaction  $^{139}\text{La}(d,p)^{140}\text{La}$ . Experimental data are represented by crosses or by an asterisk, when a background was subtracted, or by a circle when an impurity component was subtracted. A circle surrounded by an asterisk indicates that both subtractions have been performed. (a) Levels at 0, 30, 37, 49, and 63 keV, belonging to the  $(1g_{7/2})_p(2f_{7/2})_n$  configuration; (b) levels at 602, 745, and 772 keV; (c) levels at 1036, 1057, and 1077 keV; (d) levels at 1102 and 1118 keV; (e) levels at 1343 and 1352 keV; (f) levels at 1403, 1418, 1432, and 1444 keV; (g) level at 1461 keV; (h) levels at 1479, 1493, 1508, 1519, and 1529 keV; (i) levels at 1555, 1568, and 1584 keV; (j) levels at 1617, 1630, and 1644 keV; (k) levels at 1657, 1672, and 1685 keV; (l) levels at 1702 and 1718 keV; (m) levels at 1778 and 1795 keV.



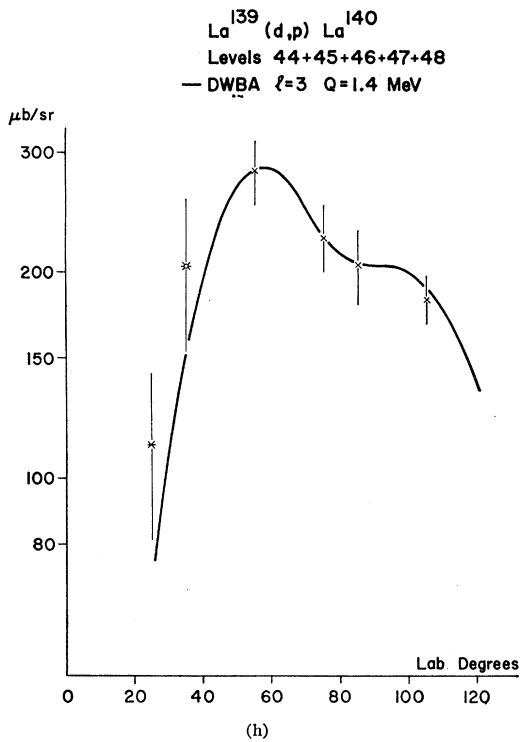
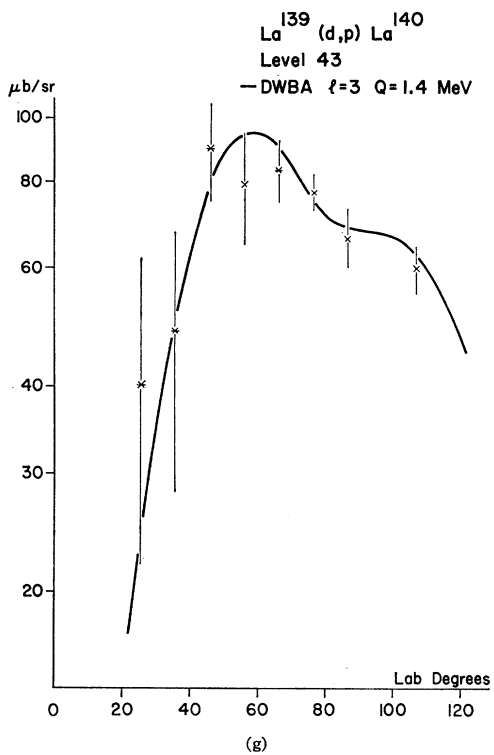
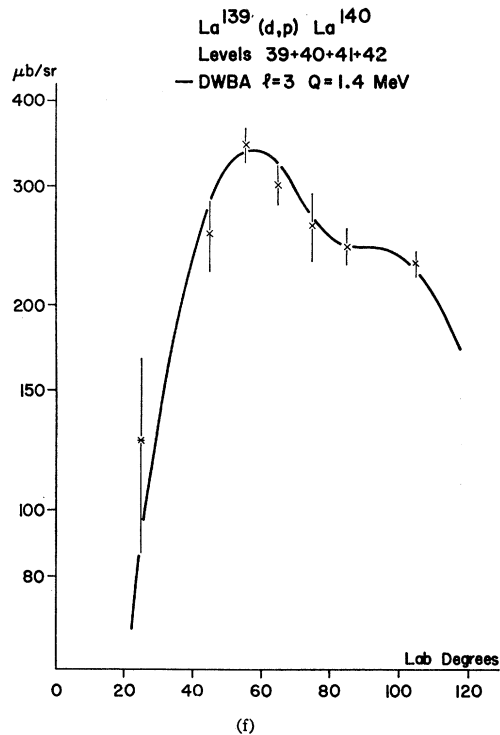
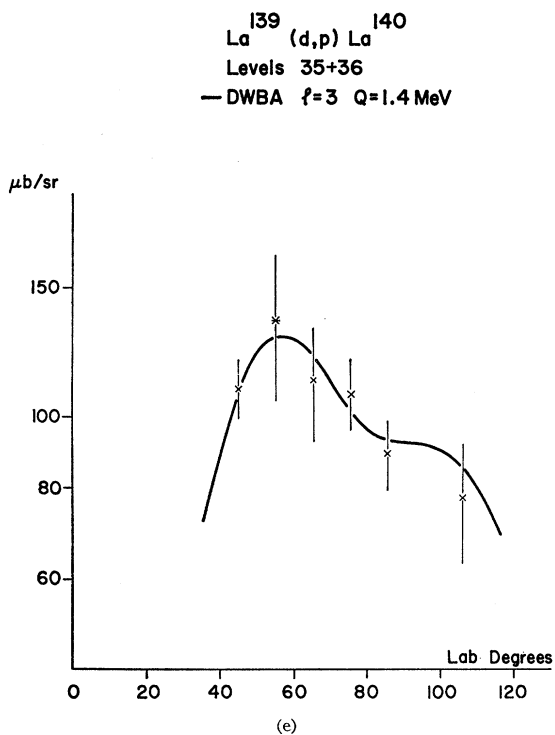


FIG. 4. (continued).

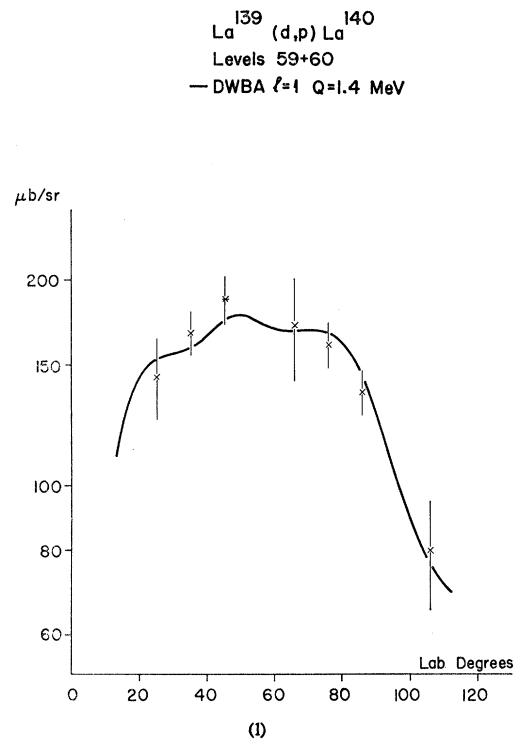
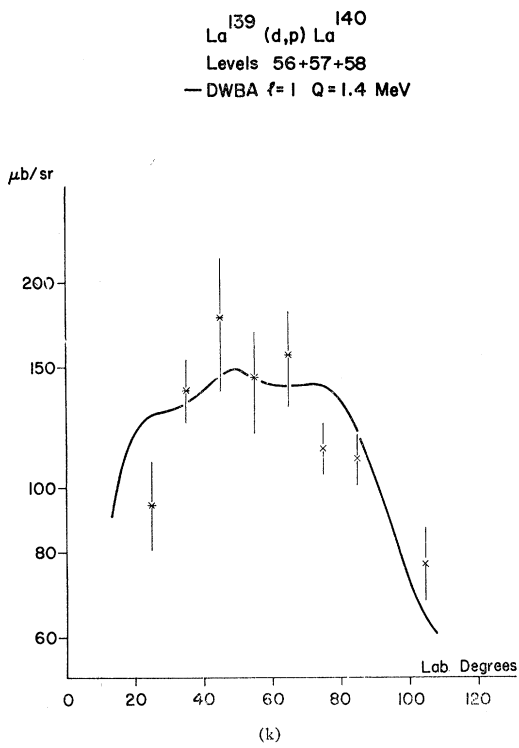
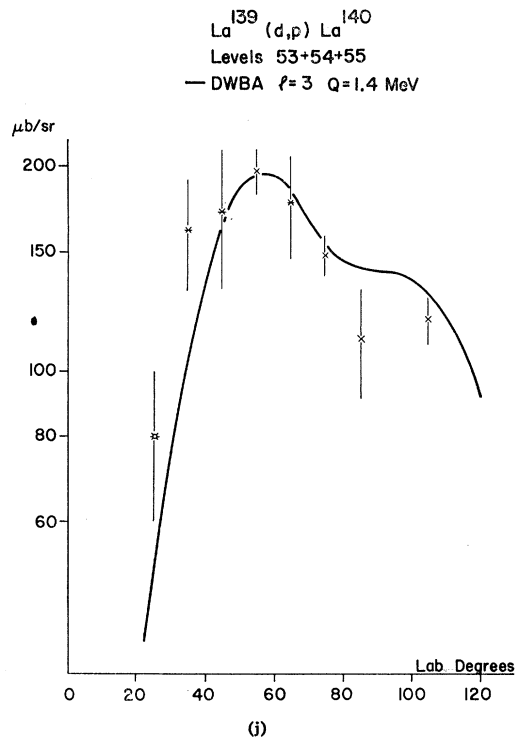
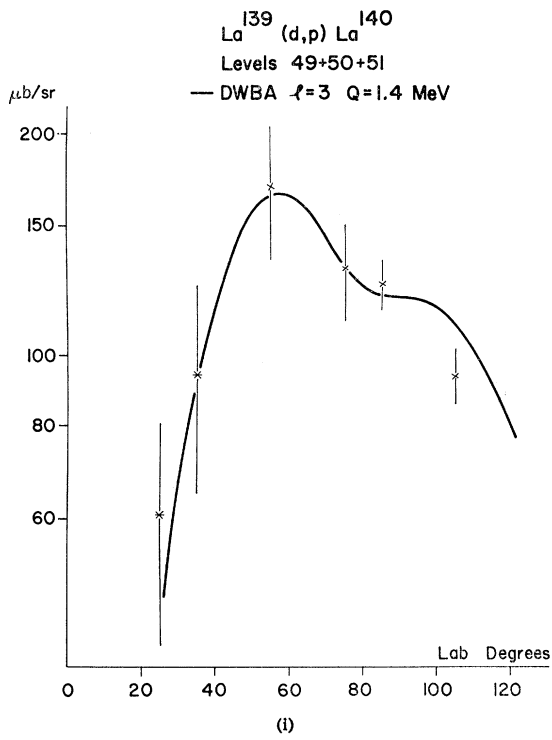


FIG. 4. (continued).

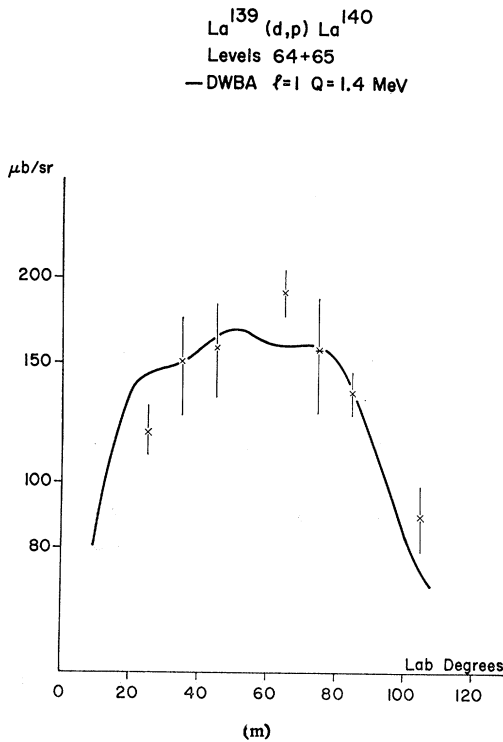


FIG. 4. (continued).

The values for the proton potential were extracted with no modifications from the work of Perey.<sup>20</sup> For the deuteron potential, we used the set of values  $A$  from Perey and Perey<sup>21</sup> and changed only the real radius (from 1.15 to 1.26 F). A lower cutoff radius of 5 F was used in the calculation.

The fit obtained is very satisfactory. It is possible that small adjustments of the optical-potential parameters compensate some of the approximations of the theory. The fact that our experimental distributions could be so well fitted is our only evidence that the reaction under study is essentially direct.

The use of the least-squares fit to analyze the data has generally resulted in little dispersion in energy values for components of unresolved multiplets. The intensities, however, often have large uncertainties. For this reason it is better, in general, to compare only the intensity sum of badly or unresolved peaks with the theoretical curves. A meaningful result is obtained

only if the  $l$  transferred is the same for each of the components. The angular distribution of such groups are plotted in Fig. 4. By a normalization of the total intensity, it is possible to compute the average relative amplitude of each component. The normalized intensities of a number of peaks belonging to different groups are given in Tables IV, V, and VI. The level diagram in Fig. 5 collects all the information on energy and  $l$  transfer obtained in this work. For an extended region, from 1130- to 1330-keV excitation, no  $l$  assignment could be obtained. We were also unsuccessful in locating levels with  $l=5$  and  $l=6$  transfer. The multiplicity of these levels should be equal to the multiplicity of the  $l=3$  levels, but their cross section should be an order of magnitude smaller. The large level density may preclude observing such states.

## V. INTERPRETATION OF RESULTS

The nucleus  $^{140}\text{La}$  with 57 protons and 83 neutrons has one neutron outside the 82 magic core. The energy-level systematics of neighboring isotonic odd- $A$  nuclei strongly suggest that this neutron occupies the  $2f_{7/2}$  orbital. Outside the 50 magic core are seven protons which are probably in the  $1g_{7/2}$  orbital. If the  $1g_{7/2}$  orbital were separated from other proton orbitals by an energy of at least 1 MeV, it might be possible to describe the low-lying states as arising from a configuration consisting of a  $2f_{7/2}$  neutron particle and a  $1g_{7/2}$  proton hole. However, in  $^{139}\text{La}$  the  $2d_{5/2}$  proton orbital appears at 166 keV of excitation. This suggests that there is strong configuration interaction in the proton system and indeed proton-proton pairing correlations seem to explain the position of this state.<sup>4</sup>

The effects of the proton-proton pairing correlations have a particularly simple physical interpretation in terms of quasiparticles. These quasiparticles are independent excitations which are hole excitations for orbitals well below the Fermi surface. They are particle excitations for orbitals well above the Fermi surface, but they have mixed particle and hole nature near the Fermi surface. The use of this independent-quasiparticle picture has had great success in quantitatively explaining many of the low-energy features of odd- $A$  and even-even nuclei in the mass region which we are considering. Its quantitative application to many odd-odd nuclei is as yet untested but qualitatively we would expect the gross structure of the odd-odd nucleus to be

TABLE III. Optical-model parameters.

	"d" potential	"p" potential
Depth of real potential $V_S$ (MeV)	73	57
Nucleus and charge radius $r_{0s}, R_C$ (F)	1.26	1.25
Diffuseness of real potential $a_S$ (F)	0.87	0.65
Depth of surface part of imaginary potential $W_D$ (MeV)	12	14
Nuclear radius of imaginary potential $r_{0I}$ (F)	1.37	1.25
Diffuseness of imaginary potential $a_I$ (F)	0.7	0.47

TABLE IV. Normalized cross sections of the peaks G.S., 1, 2, 3, 4, 5, 6, 7, 8, and 9. Norm: G.S.+1+2+3+4=100. Angular distribution:  $l=3$  [see Fig. 4(a)]. The standard deviation is given beneath each value.

Level	Energy (keV)	Normalized differential cross section ( $\mu\text{b}/\text{sr}$ )								Average
		25°	35°	45°	55°	65°	75°	85°	105°	
G.S.	0.0	15	15	11	13	15	15	13	13	13.6
		2	1	1	1	1	1	1	2	
1	30.6	12	9	16	11	17	17	17	15	14.4
		0.2	15	5	4	6	6	5	10	
2	37.5	23	29	16	26	19	18	19	21	21.2
		0.4	13	5	3	4	4	4	11	
3	49.2	31	31	34	30	29	30	29	31	30.4
		0.3	3	2	2	2	4	3	2	
4	63.2	20	16	23	21	20	21	23	21	20.5
		0.2	2	1	1	2	1	1	2	
5	161.6	7.0	4.7	6.7	5.7	5.4	5.7	6.8	5.7	6.0
		0.3	0.6	0.4	0.6	0.5	0.4	0.4	0.5	
6	284.2	34	34	36	37	34	35	39	31	35.7
		0.4	2	2	2	2	2	2	3	
7	319.2	3.9	2.3	3.0	2.3	3.0	3.2	4.3	4.2	3.3
		0.7	0.3	0.3	0.3	0.2	0.5	0.3	0.5	
8	466.6		2.4	2.6	2.7	2.3	2.4	2.3	2.3	2.40
		1.0	0.3	0.2	0.2	0.3	0.2	0.4	0.3	
9	578.6		2.1	2.9	1.4	1.2	1.3	2.4	0.8	1.7
		1.4	0.3	0.5	0.4	0.2	0.2	0.2	0.4	

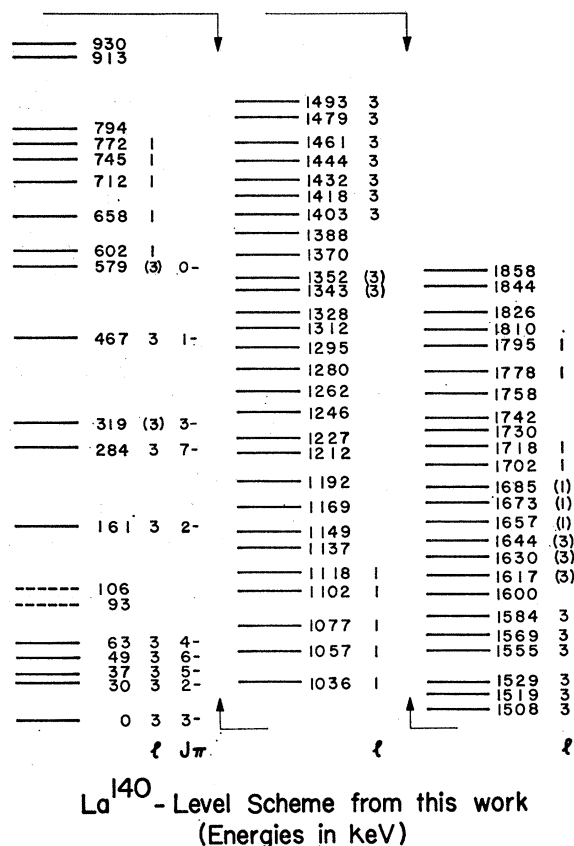


FIG. 5. Level scheme for  $^{140}\text{La}$  from these experiments. Excitation energies are in keV.

very similar to that predicted by the two-particle shell model.

For example, if we consider  $^{140}\text{La}$  and attempt to predict the lowest energy states, then there are two configurations of importance that arise from the neutron in the  $2f_{7/2}$  orbital and a quasiproton in either the  $1g_{7/2}$  orbital or the  $2d_{5/2}$  orbital. From the first configuration, we expect an octuplet of levels that have spins 0-7 and negative parity. From the second configuration, there will be a sextuplet of levels that have spins 1-6 and negative parity. The ordering of the levels within each multiplet will be different from that predicted by the two-particle (or hole) shell model since each quasiparticle is part particle and part hole. Therefore in the case of  $^{140}\text{La}$ , there are both particle-particle and particle-hole interactions. It is not surprising, then, that Brennan and Bernstein's coupling rules<sup>22</sup> are violated.

These rules predict a ground-state spin and parity of 6- for a particle-hole configuration while for a particle-particle configuration they predict a 0- ground state. However, it is believed the ground state has a spin and parity of 3-. The situation is further complicated by the fact that two configurations generating states of the same parity are very close to each other in energy. This suggests that there might be considerable configuration mixing because of the residual neutron quasiproton interaction. The  $(d,p)$  reaction is a sensitive test of this prediction. If there is no configuration interaction, then because of the well-known selection rule that proton-excited configurations are not excited by direct  $(d,p)$  reactions, the sextuplet of states

<sup>22</sup> M. H. Brennan and S. A. Bernstein, Phys. Rev. 120, 927 (1960).

TABLE V. Normalized cross sections of the peaks 10, 11, 12, 13, and 14. Norm:  $10+13+14=100$ . Angular distribution:  $l=1$  [see Fig. 4(b)]. The standard deviation is given beneath each value.

Level	Energy (keV)	Normalized differential cross section ( $\mu\text{b}/\text{sr}$ )								Average
		25°	35°	45°	55°	65°	75°	85°	105°	
10	601.6	38* <sup>a</sup>	35	33	38	39	38	38	33	36.4
	0.6	3	2	2	3	2	2	3	3	0.9
11	658.3	33*		38	41	42	39	35	42	38.5
	0.5	3		2	3	2	2	2	3	1.3
12	711.6	23*		18	23	19	17	16	19	19.1
	0.7	2		1	2	1	1	1	2	1.0
13	744.5	16*	18*	15	14	14	12	14	15	14.8
	0.7	2	2	1	1	1	1	1	1	0.6
14	711.7	46*	47*	52	49	46	50	48	52	48.6
	0.6	5	6	3	3	3	3	3	3	0.8

<sup>a</sup> The asterisk denotes that a background has been subtracted from this peak.

$|2d_{5/2}(p)2f_{7/2}(n); J\pi=1-, \dots, 6- \rangle$  will not be observed. Further, the octuplet of states  $|1g_{7/2}(p)2f_{7/2}(n); J\pi=0-, \dots, 7- \rangle$  will have intensities proportional to  $(2J+1)$ . The next states populated in the  $(d,p)$  reaction would then presumably be  $|1g_{7/2}(p)3p_{3/2}(n); J\pi=2-, \dots, 5- \rangle$ . Of course the quartet of states  $|2d_{5/2}(p)3p_{3/2}(n); J\pi=1-, \dots, 4- \rangle$  should also be close in energy and possibly mix. The states that arise from the  $2f_{7/2}$  neutron configuration should all have  $l=3$  angular distributions. Those from the  $3p_{3/2}$  configuration should have  $l=1$  angular distributions.

Finally in this qualitative discussion of the quasiparticle model, it should be pointed out that in order to explain even-even nuclei and odd- $A$  nuclei in many mass regions vibrational states must be considered. However in  $^{140}\text{La}$  we have a particularly favorable case. An examination of Kisslinger and Sorensen's  $^{139}\text{La}$  and  $^{141}\text{Ce}$  wave functions<sup>4</sup> shows that the lowest levels are essentially pure quasiparticle in nature. This results because in  $^{139}\text{La}$  (a single-closed-shell nucleus) the one-phonon quadrupole vibration is  $\sim 1.5$  MeV. In  $^{140}\text{La}$  we may hope to explain our states as pure two-quasiparticle excitations without the complication of con-

sidering collective admixtures. The analysis which follows is summarized in Table VII.

(1) Let us first consider level 6 at 284.2 keV. It is the most intense peak in the  $(d,p)$  spectrum below 600 keV of excitation and has a relative intensity of 35.7. (See Table IV.) This state has an  $l=3$  angular distribution, and is assigned as the  $|1g_{7/2}(p)2f_{7/2}(n); J\pi=7- \rangle$  state. This assignment is based on the fact that no other state with a spin and parity  $7-$  is expected in the low-energy portion of the spectra. Therefore the  $7-$  state should be very pure. According to the  $(2J+1)$  rule, this must be the most intense state in the multiplet  $|1g_{7/2}(p)2f_{7/2}(n); J\pi=0-, \dots, 7- \rangle$ . Configuration mixing in other members of this multiplet does not change this conclusion since configuration mixing can only reduce the intensities of the individual mixed states. Besides knowing that the state is pure, we see also that the peak at 284.2 keV is well-defined and its area is accurately determined. Thus we may safely use it to measure configuration mixing in other states by determining their relative intensity with respect to this state.

(2) The ground state has a spin and parity of  $3-$ . This has been deduced both from its beta decay<sup>6</sup> and

TABLE VI. Normalized cross sections of the peaks G.S., 1, 2, 3, 4, 5, 6, and 8. Norm:  $18+19+20+21+22=100$ . Angular distribution:  $l=1$  [see Figs. 4(c) and 4(d)]. The probable error is given beneath each value.

Level	Energy (keV)	Normalized differential cross section ( $\mu\text{b}/\text{sr}$ )								Average
		25°	35°	45°	55°	65°	75°	85°	105°	
18	1035.8	9* <sup>a</sup>	8	9	5	7	7	5	6	7.0
	0.6	2	1	1	1	1	1	1	1	0.6
19	1056.9	48	53	51	56	56	55	50	58	53.3
	0.8	4	4	4	4	3	3	3	3	1.2
20	1076.9	4.5	5.0	4.2	2.6	2.2	3.5	5.2	1.9	3.6
	1.4	0.4	0.8	0.6	0.6	0.6	0.8	0.4	0.4	0.4
21	1102.4	24	22	24	24	24	25	24	23	23.9
	0.9	2	2	2	2	2	2	2	2	0.3
22	1118.2	14	12	12	12*	12	9	16	10	12.3
	0.9	2	1	1	2	1	1	1	2	0.7

<sup>a</sup> The asterisk denotes that a background has been subtracted from this peak.

TABLE VII. Configuration analysis. The probable error is given beneath each value.

1	2	3	4	5	6	7	8	9	10	
Level No.	Energy (keV)	Normalized intensity	Intensity by the $(2J+1)$ rule <sup>a</sup>	Spin	Experimental state vector $\alpha$	$ \beta $	Calculated intensity	Relative experimental intensity	Comments Sec. V	
G.S.	0.0	13.6 0.5	0.47	3	0.90	0.43	0.38	0.38 0.02	2	
1	30.6 0.2	14.4 2	0.33	2	0.69	0.72	0.16	0.99 $\pm 0.04$	9	
2	37.5 0.4	21.2 2	0.73	5	1.0	$\sim 0$	0.73		0.40 0.06	11
2a	43	Unobserved	0.20	1	0.81	0.59	0.13		0.59 0.06	10
3	49.2 0.3	30.4 0.6	0.87	6	1.0	$\sim 0$	0.87	Unobserved 0.85 0.03	5	
4	63.2 0.2	20.5 0.8	0.60	4	1.0	$\sim 0$	0.60	0.58 0.03	4	
5	161.6 0.3	6.0 0.3	0.0	2	0.72	0.69	0.17	0.17 0.01	7	
6	284.2 0.4	35.7 0.6	1.00	7	1.0		1.00	1.00 0.02	1	
7	319.2 0.7	3.3 0.3	0.0	3	0.43	0.90	0.09	0.09 0.01	3	
8	466.6 1.0	2.4 0.1	0.0	1	0.59	0.81	0.07	0.07 <0.01	8	
9	578.6 1.4	1.7 0.3	0.06	0	1.0		0.06	0.05 0.01	6	

<sup>a</sup> It is assumed that for spin doublets the lower energy number belongs to the  $1g_{7/2}$  proton configuration. Column 3: From Table IV. Columns 8 and 9: Intensity of peak 6 normalized to 1.0. Column 4: Intensity for the pure  $1g_{7/2}$  configuration.

from atomic-beam studies.<sup>23</sup> This state has a measured  $l=3$  angular distribution, consistent with the neutron being in the  $2f_{7/2}$  orbital and has a relative intensity of 13.6. If the state were pure  $|1g_{7/2}(p)2f_{7/2}(n); J\pi=3- \rangle$ , then the  $(2J+1)$  rule would predict that  $(I_{3-}/I_{7-})_{\text{theor}}=0.47$ . The experimental ratio is  $(I_{0-}/I_{284.2})_{\text{expt}}=0.38\pm 0.02$ . Because of arguments given earlier in this section, let us suppose that the pairing scheme in <sup>139</sup>La is good. Then to good approximation<sup>24</sup> we need to consider only two quasiproton states in <sup>140</sup>La, viz.  $|1g_{7/2}(p)\rangle$  and  $|2d_{5/2}(p)\rangle$  so that for spins 1-6 there are only the state vectors:

$$\begin{aligned}
 |JM\rangle_1 &= \alpha_1 |1g_{7/2}(p)2f_{7/2}(n); JM\rangle \\
 &\quad + \beta_1 |2d_{5/2}(p)2f_{7/2}(n); JM\rangle, \\
 |JM\rangle_2 &= \alpha_2 |1g_{7/2}(2)2f_{7/2}(n); JM\rangle \\
 &\quad + \beta_2 |2d_{5/2}(p)2f_{7/2}(n); JM\rangle.
 \end{aligned}$$

If we choose phases so that the  $\alpha$ 's are positive, then  $\beta_1 = \pm(1-\alpha_1^2)^{1/2}$ ,  $\alpha_2 = |\beta_1|$ , and  $|\beta_2| = \alpha_1$ . In direct-reaction theory, the cross section for a state is proportional to the spectroscopic factor. For the  $(d,p)$  reaction, this is the square of the overlap integral of the target ground state plus the incident neutron and the final state in the daughter nucleus. Thus for state 1, the spectroscopic factor will be proportional to  $\alpha_1^2$

<sup>23</sup> F. R. Petersen and H. A. Shugart, Bull. Am. Phys. Soc. 5, 343 (1960).

<sup>24</sup> BCS calculations described in the second paper [G. L. Struble, Phys. Rev. 153, 1347 (1966)] predict that in <sup>139</sup>La the  $2d_{5/2}$  quasiproton state is  $\sim 200$  keV above the  $1g_{7/2}$  state but that all other states of the same parity are  $>2000$  keV.

while for state number 2, it will be proportional to  $\beta_1^2$ . The theoretical ratio of intensities for mixed states will be  $(I_{J-}/I_{7-})_{\text{theor}} = \gamma^2(2J+1)/15$  where for states labeled 1,  $\gamma = \alpha_1$  and for states labeled 2,  $\gamma = \beta_1$ . Solving this expression for  $\gamma$  using the experimental intensity ratio, we find that for the ground state  $|\alpha| = 0.90$  and  $|\beta| = 0.43$ . In fitting transition probabilities Burde *et al.*,<sup>9</sup> assume that this state is pure.

(3) If there are only two contributing configurations, then we expect a second 3- state with  $\alpha = 0.43$  and  $|\beta| = 0.90$ . The predicted relative intensity of this state is  $(I_{3-}/I_{7-})_{\text{theor}} = 0.09$ . Level 7 at 319.2 keV has an experimental relative intensity of  $(I_{3-}/I_{7-})_{\text{expt}} = 0.09 \pm 0.01$  units. On the basis of the evidence we conclude that level 7 is the second 3- state.

(4) Level 4 at 63.2 keV has a  $l=3$  angular distribution and a relative intensity of 20.5. This yields the experimental ratio  $(I_{63.2}/I_{284.2})_{\text{expt}} = 0.58 \pm 0.03$ . This is in excellent agreement with the theoretical prediction of the  $(2J+1)$  rule for an unmixed 4- state, viz.  $(I_{4-}/I_{7-})_{\text{theor}} = 0.60$ . Therefore we conclude that the state at 63.2 keV has  $J\pi = 4-$  and  $\alpha = 1.0$ . Because of its high spin, this level would not be observed in the beta decay of <sup>140</sup>Ba and since  $\alpha = 1.0$ , the second 4- state is not expected to be observed in the  $(d,p)$  experiment.

(5) Level 3 at 49.2 keV has a  $l=3$  angular distribution and a normalized intensity of 30.4. Using the  $(2J+1)$  rule for unmixed states, one would conclude that  $(I_{6-}/I_{7-})_{\text{theor}} = 0.87$ . If we take the ratio of the

relative intensity of this level and the  $7-$  level, we find that  $(I_{49.2}/I_{284.2})_{\text{expt}}=0.85\pm 0.03$ . Considering the experimental errors, this is sufficiently close to the theoretical ratio to conclude that the 49.2-keV level has  $J\pi=6-$  and  $\alpha=1.0$ . Here also the large spin of this state precludes its observation in the beta decay of  $^{140}\text{Ba}$ , and since  $\alpha=1.0$ , the second  $6-$  state should not be observed in the  $(d,p)$  experiment.

(6) Level 9 at 578.6 keV corresponds to the level observed in beta decay of  $^{140}\text{Ba}$ .<sup>7,9</sup> at 580 keV. This level has tentatively been assigned  $0-$  spin and parity. This state, like the  $7-$  state, should be essentially pure. Because of its very small intensity, it was not feasible to measure its angular distribution. However its normalized intensity is 1.7 so that  $(I_{578.6}/I_{284.2})_{\text{expt}}=0.05\pm 0.01$ . The theoretical value for the unmixed  $0-$  state is  $(I_{0-}/I_{7-})_{\text{theor}}=0.067$ . This agreement strongly supports the spin-0 assignment.

(7) Level 5 at 161.6 keV has also been observed in the beta decay of  $^{140}\text{Ba}$ .<sup>7-9</sup> The 162-keV transition to the ground state is almost entirely  $M1$  and so the fact that it has been populated directly in the beta decay of  $^{140}\text{Ba}$  makes the spin and parity assignment of  $2-$  unique. This state has an  $l=3$  angular distribution and a normalized intensity of 6.0. Therefore for this state  $\alpha=0.72$  and  $|\beta|=0.69$ . This would imply that the normalized intensity of the second  $2-$  state is 5.7. Burde *et al.*<sup>9</sup> have also found that the  $2-$  states are highly admixed.

(8) Level 8 at 466.6 keV has been observed in the beta decay of  $^{140}\text{Ba}$ .<sup>7-9</sup> Both angular-correlation measurements and measurements of the mean life of the state<sup>9</sup> suggest that it has  $J\pi=1-$ . This level has an angular distribution consistent with  $l=3$  and a normalized intensity of 2.4. This yields the experimental ratio  $(I_{466.6}/I_{284.2})_{\text{expt}}=0.07\pm 0.01$  while the theoretical ratio from the  $(2J+1)$  rule for unmixed states is 0.20. Therefore  $\alpha=0.59$  and  $|\beta|=0.81$ . This is in contrast to the results of Burde *et al.*<sup>9</sup> who argue from transition probabilities that the two  $1-$  states are only slightly admixed. The normalized intensity of the second  $1-$  state is predicted to be 4.6 units.

(9) Level 1 at 30.6 keV is certainly the state observed in the decay of  $^{140}\text{Ba}$  at 29.6 keV.<sup>7-9</sup> The 29.6-keV gamma transition to the ground state is predominantly  $M1$  and so the fact that it is observed in beta decay from the  $0+$  ground state of  $^{140}\text{Ba}$  makes the spin assignment of  $2-$  unique. This state has an  $l=3$  angular distribution and a relative intensity of 14.4. The predicted value for the normalized intensity of this state (see paragraph 7) is only 5.7. But even if this state were pure, the  $(2J+1)$  rule would predict a normalized intensity of only 11.8 units. Clearly this is impossible and indicates that there are either more levels in the first group of peaks than the least-squares analysis indicates and/or there is not sufficient experimental detail to accurately determine the relative

intensities of the states labeled 1 and 2. This is suggested by the fact that an acceptable fit in the least-squares sense can be obtained by omitting peak 1 and that there appears to be a large systematic error in the excitation energy measured in the  $(d,p)$  experiment.

(10) From the beta decay of  $^{140}\text{Ba}$ ,<sup>7-9</sup> it is deduced that there is a state at 43 keV. The fact that it does not decay to the ground state strongly suggests that its spin and parity are  $1-$ . We find no state at 43 keV. However if the state were pure  $|2d_{5/2}(p)2f_{7/2}(n); J\pi=1-\rangle$ , then it would not be excited in the  $(d,p)$  reaction. Assuming that the values of  $\alpha$  and  $|\beta|$  extracted in (8) are an accurate measure of the mixing of these two states, then we would expect a normalized intensity for this  $1-$  state of 4.6 units. Although our experimental detail is insufficient to define this peak, its arbitrary inclusion helps to explain the discrepancies cited in paragraph (9).

(11) We have now accounted for seven of the eight states expected from the multiplet  $|1g_{7/2}(p)2f_{7/2}(n); J\pi=0-, \dots, 7-\rangle$ . Only the  $5-$  state is missing. This state cannot be observed in the beta decay of  $^{140}\text{Ba}$ , and if it is unmixed, the  $(2J+1)$  rule predicts that its normalized intensity should be 26.1. Level 2 has a normalized intensity of 21.2. Rather than propose that this decreased intensity is due to configuration mixing, it seems more likely that states 1 and 2, in addition to the unobserved state at 43 keV, are inadequately decomposed by the least-squares analysis. From arguments presented in paragraph (9), there are 8.7 too many units of normalized intensity in level 1. Of these, 4.9 units can be accounted for if level 2 has 26.1 units of intensity. An additional 4.6 units would be accounted for if the mixing of the  $1-$  states deduced in paragraph (10) is correct. Thus within experimental accuracy, we have accounted for the intensity within the first group of peaks by assuming that the  $5-$  state is unmixed and that the intensity of the  $2-$  and  $1-$  states in this group can be predicted from a knowledge of the relative intensities of the 162-keV  $2-$  state and the 467-keV  $1-$  state. Since we have assigned the value  $\alpha=1$  for this state, we expect not to observe the second  $5-$  state in the  $(d,p)$  experiment.

(12) Peaks 10-14 are five intense, well-resolved peaks having  $l=1$  angular distributions and a mean energy of 687 keV. From the systematics of neighboring isotonic odd- $A$  nuclei, one expects that the  $3p_{3/2}$  neutron orbital should appear at  $\sim 700$  keV in excitation. If we assume that we can neglect vibrational states, then there should be eight states produced from the configurations

$$|1g_{7/2}(p)3p_{3/2}(n); J\pi=2-, \dots, 5-\rangle$$

and

$$|2d_{5/2}(p)3p_{3/2}(n); J\pi=1-, \dots, 4-\rangle.$$

To first order, the states having spins 2, 3, and 4 may be close enough in energy so that they can be appreciably mixed. Of course, the  $|1g_{7/2}(p)3p_{3/2}(n); J\pi=5-\rangle$  state would be pure and should be the most intense.

But the method of analysis used in paragraphs (1)–(11) fails. After summing the total  $l=1$  intensity of these five peaks, we find that peak 14, the most intense of this group, is six units too small in relative intensity to be the  $5-$  state predicted by the  $(2J+1)$  rule. This suggests that here phonon admixtures are appreciable. This is not surprising since Fulmer *et al.*,<sup>25</sup> found appreciable phonon mixing for the  $3p_{3/2}$  state in  $^{141}\text{Ce}$ . It is pertinent that in  $^{141}\text{Ce}$ , a nucleus with only one more proton, Fulmer *et al.*<sup>25</sup> find the  $3p_{3/2}$  strength shared between levels at 660 and 1120 keV and that the mean energies of our first two groups (levels 10–14 and levels 18–22) that have  $l=1$  angular distributions are 687 and 1077 keV. Fulmer *et al.*<sup>25</sup> see their first excited state which has an  $l=3$  angular distribution at 1500 keV. We observe a sequence of levels that have  $l=3$  angular distributions between 1400 and 1600 keV which we therefore attribute to states having a large single-particle  $2f_{5/2}$  component in their state vector. Fulmer *et al.*<sup>25</sup> observe their first  $l=1$  state attributable to the  $3p_{1/2}$  single-particle state at 1730 keV. We observe a sequence of states having  $l=1$  angular distributions between 1702 and 1795 keV.

It becomes very complex to discuss these states in terms of even a simple odd-odd quasiparticle and phonon model because the state vector is then a linear combination of the basis vectors  $|\vec{j}_p \vec{j}_n J; pR; IM\rangle$ , where  $\vec{j}_p$  and  $\vec{j}_n$  are the quantum numbers of the quasiprotons and neutrons which couple to angular momentum  $J$ . The letter  $p$  represents the number of phonons coupled to angular momentum  $R$ , and  $J$  and  $R$  are coupled to  $I$ . Even if we restrict our analysis to states with at most one phonon ( $pR=00$  and  $12$ ) and with  $\vec{j}_p=1g_{7/2}$  or  $2d_{5/2}$  and  $\vec{j}_n=2f_{7/2}$  or  $3p_{3/2}$ , there are 17 basis vectors having that spin 5 and negative parity. At least five of these will be close enough in zeroth order to couple extensively with the  $|(1g_{7/2}3p_{3/2})5; 00; 5\rangle$  component which has the total  $3p_{3/2}$  strength for spin-5 states. This complexity in the nuclear structure makes it impossible to use simple relationships such as the  $(2J+1)$  rule and angular distributions to deduce detailed information about the nature of the states or even as measure of their spin.

## VI. CONCLUSION

We have observed 70 levels below 1.858 MeV in the nucleus  $^{140}\text{La}$  by  $(d,p)$  reaction spectroscopy and have

<sup>25</sup> R. H. Fulmer, A. L. McCarthy, and B. L. Cohen, Phys. Rev. **128**, 1302 (1962).

characterized 43 of them by specifying their  $l$  values as deduced from angular distributions. Of the 14 lowest levels expected from the two configurations

$$|1g_{7/2}(p)2f_{7/2}(n); J\pi=0-, \dots, 7-\rangle$$

and

$$|2d_{5/2}(p)2f_{7/2}(n); J\pi=1-, \dots, 6-\rangle,$$

we have characterized 11 with respect to their energy position, spin, parity, and the absolute value of the amplitudes in the state vectors with the assumption that configurations other than the two mentioned above are not important. In addition, the  $(d,p)$  intensity of the observed  $4-$ ,  $5-$ , and  $6-$  states suggest that they are not appreciably mixed and therefore the three unobserved states which also have these spins should be observed in the  $(d,p)$  experiment with very small intensity. Below 600 keV we have not been able to interpret the two weak levels  $4b$  and  $4c$ . However, as shown in Table II, only one of these peaks may be real. It is most likely the unassigned  $4-$ ,  $5-$ , or  $6-$  state and is populated either through a weak  $1g_{7/2}$  proton component or a second-order process in the  $(d,p)$  reaction. Any attempt to extend these simple interpretations to levels above 600 keV seems doomed because of the strong phonon-particle coupling.

$^{140}\text{La}$  is one of the first nonmagic vibrational odd-odd nuclei to be carefully studied. The results suggest, at least qualitatively, the validity of the odd-odd quasiparticle model, but above 500 keV careful consideration of the particle-phonon interaction must be included in any description even in this simple case where there are only 83 neutrons.

## ACKNOWLEDGMENTS

The authors wish to acknowledge a critical reading of the manuscript by John Rasmussen and valuable comments by Professor Rasmussen and Dr. T. Udagawa. The assistance of Carson Nealy, Frank Rickey, and the crew of the F. S. U. Tandem Van de Graaff in taking the data, and the careful plate-counting of Mary Jones, Sue Hipps, and Ella Jean Wehunt are greatly acknowledged. One of us (J. K.) wishes to thank IBM International (Extension Suisse) for five free hours on the IBM 7040 computer at the Polytechnic School in Lausanne.